

STUDY ON THE INHERENT SAFETY OF ON-BOARD METHANOL REFORMING HYDROGEN PRODUCTION FUEL CELL SYSTEM

Zijian, Deng.¹, Mingqi, Bai.², Qu, Haowen.³, and Yi, Liu.⁴

¹ College of Mechanical and Electrical Engineering, China University of Petroleum (East China), Qingdao, 266580, China, dengzinjiann12@163.com

² College of Chemistry and Chemical Engineering, China University of Petroleum (East China), Qingdao, 266580, China, baimingqi867@qq.com

³ College of Chemistry and Chemical Engineering, China University of Petroleum (East China), Qingdao, 266580, China, 1073687000@qq.com

⁴ College of Chemistry and Chemical Engineering, China University of Petroleum (East China), Qingdao, 266580, China, liuyi@upc.edu.cn

ABSTRACT

Methanol as a liquid phase hydrogen storage carrier has broad prospects. Although the on-board methanol reforming hydrogen fuel cell system (MRFC) has long been proposed to replace the traditional hydrogen fuel cell vehicle, the inherent safety of the system itself has rarely been studied. This paper adopted the improved method of Inherently Safer Process Piping (ISPP) to evaluate the pipeline inherent safety of MRFC. The process data such as temperature, pressure, viscosity, and density were obtained by simulating the MRFC in ASPEN HYSYS. The Process Stream Characteristic Index (PSCI) and risk assessment of jet fire and vapor cloud explosion was carried out for the key streams with those simulated data. The results showed the risk ranks of different pipelines in the MRFC and the countermeasures were given according to different risk ranks. Through the in-depth study of the evaluation results, this paper demonstrates the risk degree of the system in more detail and reduces the fuzziness of risk rating. By applying ISPP to the small integrated system of MRFC, this paper realizes the leap of inherent safety assessment method in the object and provides a reference for the inherent safety assessment of relevant objects in the future.

1.0 INTRODUCTION

As the global environment becomes increasingly terrible, it is urgent to create an ideal carrier that served as an energy medium. Hydrogen is currently the most likely energy carrier to replace current hydrocarbons. With the development of hydrogen production technology, the commercialization of a large-scale hydrogen economy has become a viable option. Hydrogen does not contain carbon, in contrast to hydrocarbons, therefore the absence of greenhouse gases in the final product reduces the greenhouse gas emission. Significant research has been done on hydrogen production technologies, which at the moment include electrolysis, photolysis, bio-hydrogen, pyrolysis, chemical hydrogen production, and nuclear hydrogen production[1], to fully utilize the environmentally friendly and non-polluting nature of hydrogen. Hydrogen production from hydrocarbons is still a significant source of hydrogen in today's world even though many other methods exist. Nevertheless, more scientific advancements are still required and many of them are costly to implement. Currently, 50% of the world's hydrogen comes from methane steam reforming (SMR), 30% from oil/naphtha reforming, 18% from coal gasification, 3.9% from water electrolysis, and 0.1% from other sources[2].

The use of vast amounts of fossil fuels has exacerbated global climate change to some extent, resulting in global warming, air pollution, and the depletion of the ozone layer. The modern transportation industry continues to utilize a lot of fossil fuels. In addition, as people's living standard is increasing, the number of vehicles using fossil fuels is increasing globally. With increasing environmental protection awareness, hydrogen fuel cell vehicles are gradually coming into the limelight. Conventional hydrogen-fueled vehicles have been difficult to implement among the general public due to the high risk and imperfection of hydrogen refueling infrastructure. Plenty of accidents in hydrogen-related infrastructure happened around the world. In May 2019, an explosion occurred in a hydrogen fuel storage tank in South Korea, which increased distrust in the safety of hydrogen fuel cell vehicles. In June 2019, an explosion occurred at a hydrogen refueling station in Norway. Although the accident

did not directly affect hydrogen fuel cell vehicles, it still causes a certain negative impact on such vehicles, resulting in Toyota and Hyundai stopping selling hydrogen fuel cell vehicles in Norway. Therefore, a methanol-to-hydrogen fuel cell on-board system has been proposed. This system has improved the vehicle's safety because it adds methanol online hydrogen production to the vehicle. The main reaction pathways concerning methanol to hydrogen include methanol steam reforming (SRM), partial oxidative reforming of methanol (POM), oxidative steam reforming of methanol (OSRM), and adsorption-enhanced steam methanol reforming [3]. Meanwhile, different systems are equipped with different types of fuel cells, and six main types of fuel cells are used for starting electricity [4]. Chein et al. [5] designed and tested a small-scale hydrogen production reactor integrating heat supply, fuel gasification, methanol steam reforming, and carbon monoxide reforming and removal units. Furthermore, they innovatively designed and tested an integrated miniature tubular quartz reactor for hydrogen production. Kolb et al. [6] designed, fabricated, and tested a methanol reformer for high-temperature proton exchange membrane fuel cell hydrogen production for mobile applications using microstructured plate heat exchanger technology and a new highly active catalyst formulation for oxidative steam reforming of methanol at temperatures over 300°C. Yang et al. [7] developed a self-sustaining, complete, and miniaturized methanol fuel processor based on modular integration and microreactor technology. The fuel processor consists of a methanol oxidation reformer, a methanol burner, and a two-stage CO preferential oxidation unit. This unit is sufficient to supply a 1 kW proton exchange membrane fuel cell. Ghodba et al. [8] investigated the integrated design and operation of a mobile power generation system consisting of a microreactor reformer and a proton exchange membrane fuel cell (PEMFC) by taking advantage of various advantages of process miniaturization, where hydrogen fuel is provided through autothermal steam reforming of methanol in the microreactor, resulting in safer, more efficient, and more economical operation. The above are all studies on methanol to hydrogen fuel cell systems, and after finishing, the system now has seven configurations, as illustrated in Table 1.

Table 1. Methanol to Hydrogen Fuel Cell Systems

Methanol to Hydrogen Fuel Cell Systems
water vapor reforming + membrane separation technology
autothermal reforming + high-temperature proton exchange membrane fuel cell
water vapor reforming + carbon monoxide selective methanation
autothermal reforming + carbon monoxide selective oxidation
water vapor reforming + carbon monoxide selective oxidation
water vapor reforming + variable pressure adsorption
water vapor reforming + high-temperature proton exchange membrane fuel cell

Despite a large number of studies on on-board methanol reforming hydrogen production fuel cell systems, very little research has been done so far on its inherent safety. Since the system is in the early stages of development and the overall framework is still not finalized, this stage is very suitable for inherent safety analysis. The idea of inherent safety has been developed for a considerable period since it was proposed in the 1970s. During this period, many evaluation methods in terms of inherent safety have been proposed one after another. Park et al [9] divided the methods into three categories based on hazards, risks, and costs by reviewing 73 inherent safety evaluation methods, and analyzed these three different categories in detail. Despite the existence of many kinds of inherent safety evaluation methods, different methods have more or fewer limitations in applicability. Khan and Amyotte proposed the I2SI evaluation method [10], but this method only works on hazard reduction, not risk reduction, and is less flexible when applied to different stages of the process design life cycle [11]. Therefore, based on this method Rathnayaka et al.[11] proposed the RISI method to compensate for the deficiencies of the I2SI method. Chan and Shariff proposed a new method called the process route index (PRI), an index method that can be used to assess the explosion hazard of process lines, which can be calculated by assessing the explosion levels of different processes and thus determine the level of inherent safety between different processes [12]. Shariff and Leong et al. proposed an evaluation

method called process flow index (PSI) based on a single process, which derives the hazard ranking of different streams in a process by comparing them in a single process [13]. Due to the particularity of the vehicle-mounted methanol reforming hydrogen fuel cell system, and the difficulty in obtaining data from different technical routes, the PSI evaluation method has strong applicability for the existing evaluation work through comprehensive comparison. In this paper, the inherent safety assessment of the on-board methanol reforming hydrogen fuel cell system is carried out. The assessment result is expressed by the risk level, which provides a reference for the safety design of the system

2.0 METHODOLOGY

Inherent Safer Process Piping (ISPP) [14] was used and improved in this study. The related frameworks are shown in Fig. 1. The whole framework contains two main parts, which are the identification of critical process streams and the risk assessment and analysis of potential significant fire and explosion consequences of critical streams.

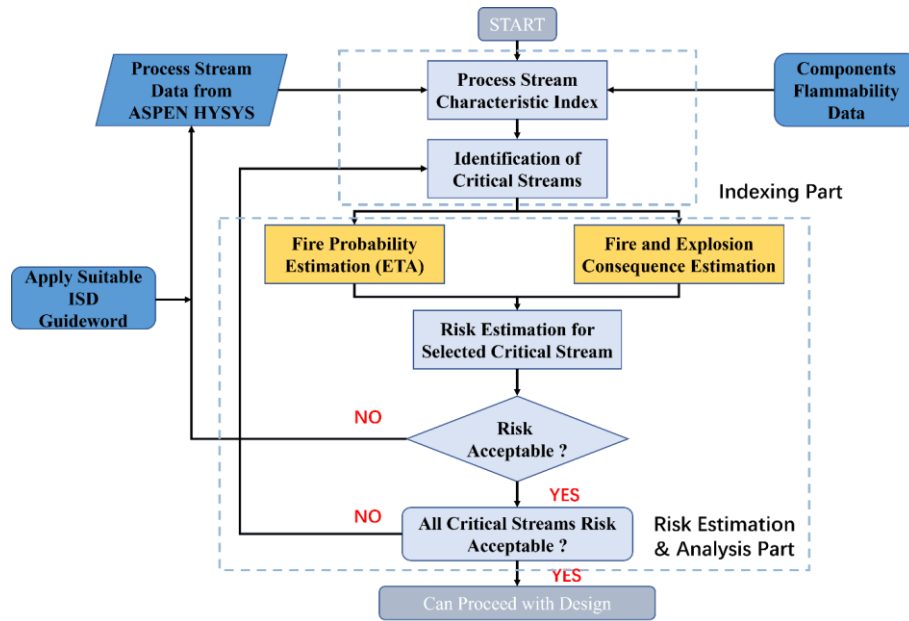


Figure 1. The improved Inherent Safer Process Piping (ISPP)

2.1 Process stream characteristic index (PSCI)

In the preliminary design phase, where data availability is limited, process streams can be considered process pipelines [13]. Previously, the process stream index (PSI) was developed to evaluate and prioritize process streams to avoid potential accidents caused by explosions. However, the issues related to flow in process piping, which is one of the causes of process piping failures, were not considered in PSI. Therefore, the PSI relationship was extended to include and evaluate the viscosity of individual streams in the process piping during the preliminary design and renamed to Process Stream Characteristic Index (PSCI), with the function expressed as

$$\text{PSCI} = f(\text{mass, phase, energy, combustibility}) \quad (6)$$

Where temperature and pressure together determine the phase state of the fluid in the processing pipeline, energy can be defined by the low heating value (LHV), and flammability can be determined from the upper and lower flammability limits. The flammability can be estimated using the following equation.

$$\text{UFL}_{\text{mix}} = \frac{1}{\sum_{i=1}^n \frac{y_i}{\text{UFL}_i}}, \quad (7)$$

$$LFL_{\text{mix}} = \frac{1}{\sum_{i=1}^n \frac{y_i}{LFL_i}}, \quad (8)$$

$$\Delta FL = UFL_{\text{mix}} - LFL_{\text{mix}}, \quad (9)$$

where UFL - upper explosion limit; LFL - lower explosion limit; y_i - molar fraction of component; ΔFL – combustibility.

Eq. (6) can subsequently be rewritten as

$$PSCI = f(\text{pressure, temperature, density, viscosity, heating energy, flammability}) \quad (10)$$

For the prioritization of streams, the concept of relative ranking of PSCI was developed based on the basic principles of the technique [14]. The streams are ranked according to the stated attributes using the following equation.

$$I_p = \frac{\text{Pressure of individual stream}}{\text{Average pressure of all streams}} \quad (11)$$

$$I_T = \frac{\text{Temperature of individual stream}}{\text{Average temperature of all streams}} \quad (12)$$

$$I_\rho = \frac{\text{Density of individual stream}}{\text{Average density of all streams}} \quad (13)$$

$$I_v = \frac{\text{Viscosity of individual stream}}{\text{Average viscosity of all streams}} \quad (14)$$

$$I_e = \frac{\text{Heating energy of individual stream}}{\text{Average heating energy of all streams}} \quad (15)$$

$$I_{FL} = \frac{\Delta FL \text{ of individual stream}}{\text{Average } \Delta FL \text{ of all streams}} \quad (16)$$

All flows in the process route of pressure, temperature, density, viscosity, and LHV values were simulated by ASPEN HYSYS. UFL and LFL values can be obtained from the literature. ASPEN HYSYS can import five parameters into MS Excel, and parameters from the literature can be inserted directly by the user, resulting in the correlation of the six indexes of the PSCI as

$$PSCI = A \times (I_p \times I_T \times I_\rho \times I_v \times I_e \times I_{FL}) \quad (17)$$

The higher the PSCI rating, the greater the damage caused by loss of containment through the process piping, which could result in fires and accidents. This index can be used to identify the most critical process piping.

2.2 Jet fire risk assessment module

For the selection of subcategories of fire scenarios, the jet fire was selected as an example of pipeline fire risk modelling. The risk of the final fire is determined by a combination of fire consequences and frequency together. The consequences of a fire depend on the intensity of radiation, which is at the same time a function of the number of chemical leaks initially released. The number of chemical leaks is directly related to the working pressure of the pipe.

The release rate of the liquid is

$$m_L = C_D A_h \sqrt{2\rho\Delta p}, \quad (18)$$

where m_L - liquid mass flow rate, kg/s; C_D - discharge coefficient; A_h - opening area, m²; ρ - density, kg/m³; Δp - operating and ambient pressure difference, kPa.

The vapor release rate under blocking conditions is

$$m_V = C_D A_h \sqrt{\gamma \rho p \left(\frac{2}{\gamma+1}\right)^{\frac{\gamma+1}{\gamma-1}}}, \quad (19)$$

where m_V - vapor mass flow rate, kg/s; γ - ratio of specific heat capacities, C_p/C_v .

The vapor release rate under non-blocking conditions is

$$m_V = C_D A_h \sqrt{2 \rho p \left(\frac{\gamma}{\gamma-1}\right) \left[\left(\frac{p_{amb}}{p}\right)^{\frac{2}{\gamma}} - \left(\frac{p_{amb}}{p}\right)^{\gamma+\frac{1}{\gamma}} \right]}, \quad (20)$$

where p_{amb} – ambient pressure, kPa.

The level of consequences of a jet fire can be determined by the intensity of radiation, as estimated by the following equation. The following equations represent the flame height, radiation path length, point view source factor, and radiation intensity, respectively.

$$\frac{L}{d} = \frac{15}{C_T} \sqrt{\frac{M_a}{M_f}}, \quad (21)$$

where L - length of the flame measured from the break point, m; d - diameter of the opening, m; C_T - fuel mole fraction concentration; M_a - molecular weight of the air, kg/kgmol; M_f - molecular weight of the fuel, kg/kgmol.

$$x = \sqrt{(s)^2 + (r)^2}, \quad (22)$$

where x - radiation path length, m; s - height of flame centre from ground, m; r - distance of interest from flame, m.

$$F = \frac{1}{4\pi x^2}, \quad (23)$$

where F - point source view factor.

$$E_r = \tau_a \eta m \Delta H_C F_p, \quad (24)$$

where E_r - radiant flux at the receiver, kJ/m²s; τ_a - atmospheric transmissivity; η - fraction of total energy converted to radiation; m - mass flow rate, kg/s; ΔH_C - energy of combustion of the fuel, kJ/kg; F_p - point source view factor.

Once the consequences of a jet fire have been calculated, it is necessary to calculate the frequency of occurrence of the scenario, which can be done through an incident tree analysis (FTA), and the incident tree modelling of the incident scenario is represented in Fig. 2. The main equation for fire frequency estimation is as follows.

$$f = [f_{IL} \times P_{imm,ign}] + [f_{IL} \times (1 - P_{imm,ign}) \times (P_{del,ign}) \times (1 - P_{exp/g/ign})], \quad (25)$$

where f_{IL} - initial leakage frequency, yr⁻¹; $P_{imm,ign}$ – probability of immediate ignition; $P_{del,ign}$ – probability of delayed ignition; $P_{exp/g/ign}$ - probability of delayed ignition leading to explosion.

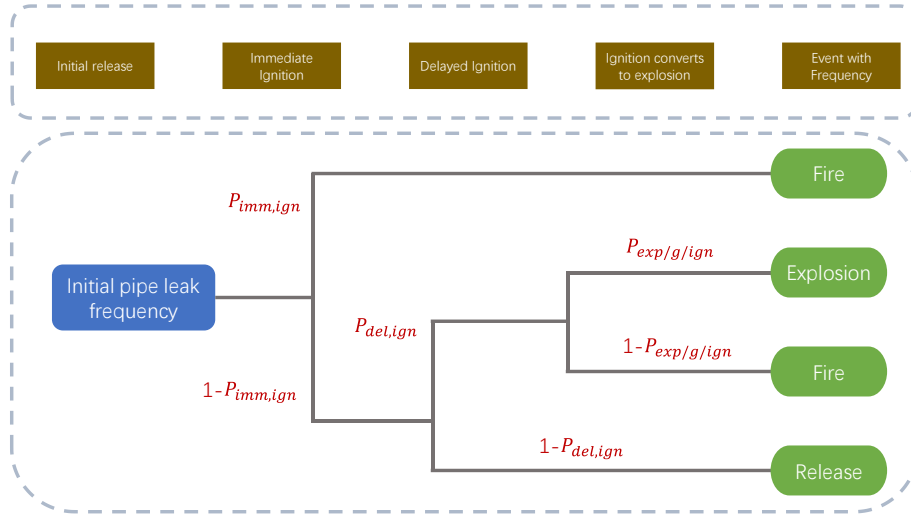


Figure 2. Event tree model with different accident consequences

2.2 Vapor cloud explosion risk assessment module

Compare with jet fires, the severity of the consequences of the accident is determined by the explosion overpressure generated by the VCE. Explosion overpressure is a function of the initial release, process, and environmental conditions. The amount of chemical released depends on the process conditions and equipment type, as each pipeline contains specific inventory levels. For small leaks, the release rate can be estimated, while for a complete rupture of the pipeline, the inventory of the equipment is usually assumed to be the mass released. For a given orifice size, the leak volume is calculated by the Eq. (19) mentioned above. The next step is to estimate the combustible mass of the released combustible vapor cloud, which is a contributing factor to the overpressure, as follows.

$$\frac{m_f}{m} = \exp \left[\sqrt{\ln \frac{c_o}{c_{LFL}}} \right] - \frac{2c_{LFL}}{c_o \sqrt{\pi}} \sqrt{\ln \frac{c_o}{c_{LFL}}}, \quad (26)$$

where m_f - flammable mass, kg; m - total mass, kg; c_o - maximum leakage concentration; c_{LFL} - lower flammability limit.

The explosion overpressure also depends on the energy released by the explosion and the scalar distance, the process then uses the TNT equivalent method to estimate these parameters, the necessary calculation equations are as follows.

$$m_{TNT} = \frac{\eta_{ex} m_f H_V}{H_{V,TNT}}, \quad (27)$$

where m_{TNT} - TNT equivalent mass, kg; η_{ex} - efficiency factor; H_V - energy of flammable mass combustion, kJ/kg; $H_{V,TNT}$ - energy of TNT combustion.

$$\bar{z} = \frac{z}{(m_{TNT})^{1/3}}, \quad (28)$$

where \bar{z} - scaled distance, m; z - distance, m.

The overpressure was estimated by a nonlinear regression of the experimental data, and the regression equation for the overpressure is shown below.

$$p_{ovr} = a_1 (b_1)^{(1/\bar{z})} z^{c_1}, \quad (29)$$

where a_1 - constant for overpressure; b_1 - constant for overpressure; c_1 - constant for overpressure;

The estimation method for VCE was also estimated using the same event tree analysis as the ISPP method, and unlike jet fire, by referring to Figure 3, the VCE was calculated as follows.

$$f = f_{IL} \times (1 - P_{imm,ign}) \times P_{del,ign} \times P_{exp/g/ign} \quad (30)$$

2.0 RESULTS AND DISCUSSION

The main findings of this study are divided into HYSYS simulation of MRFC, PSCI index ranking, critical stream risk analysis, and discussion. Firstly, the HYSYS of MRFC was introduced to understand the structure related to the study object, and the subsequent data was obtained through its simulation. Subsequently, the PSCI index was calculated using the HYSYS data to determine the critical streams. The risk analysis was then performed on the identified key streams, and the final calculated risk was represented by a risk matrix. Finally, different streams were analyzed and discussed according to different risk levels.

2.1 Research Object

The object of this paper is a highly integrated small system which can be concentrated in the vehicle. The system can simultaneously reform methanol during vehicle operation to provide a mixture containing hydrogen to the vehicle. A flow chart of the system is shown in Fig. 3.

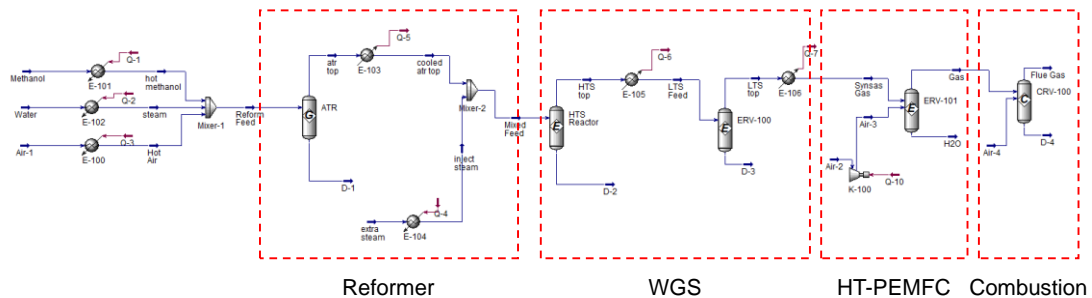


Figure 3. HYSYS simulation of MRFC

2.2 PSCI Ranking

Parameters such as temperature, pressure, low calorific value, viscosity, density, etc. can be output through HYSYS simulation. Since the flammability of the pipeline cannot be output in HYSYS, the relevant literature needs to be consulted. In all streams, some of them do not have material flow, so the irrelevant streams are removed in the analysis process. Moreover, in the feed section, the accident scenario of jet fire in the ISPP method could not be formed because the methanol was at room temperature and pressure. Finally, the PSCI index is calculated and the data is represented in Table 2.

Table 2. PSCI ranking results

Stream Name	I_p	I_T	I_c	I_v	I_p	I_{FL}	PSCI
Atr top	2.7097	1.9845	1.0704	0.3731	0.0041	1.6840	1.4765
Hot methanol	0.5139	1.9845	7.1802	0.0839	0.0184	0.7058	0.7972
Reform feed	0.5119	1.9845	1.8502	0.1675	0.0160	0.7058	0.3551
HTS top	1.1569	0.7277	0.9353	0.2180	0.0027	1.7162	0.0801
Gas	2.4764	0.7277	0.3685	0.3586	0.0019	1.6881	0.0764
Cooled atr top	0.8992	0.7277	1.0704	0.2000	0.0032	1.6840	0.0753
Mixed Feed	0.8992	0.7277	0.9760	0.1963	0.0032	1.6840	0.0667
LTS top	0.5443	0.7277	0.9234	0.1632	0.0041	1.7241	0.0418
LTS Feed	0.4625	0.7277	0.9353	0.1556	0.0043	1.7162	0.0365
Synsas Gas	0.4239	0.7277	0.9234	0.1518	0.0045	1.7241	0.0335

Stream Name	I_p	I_r	I_e	I_v	I_p	I_{FL}	PSCI
Flue Gas	3.1022	0.6701	0.1040	0.4388	0.0016	1.7246	0.0258
Steam	0.5139	1.9845	0	0.1342	0.0103	0	0
Extra steam	0.0514	0.6701	0	8.3584	7.4518	0	0
Inject steam	0.8992	0.7277	0	0.1862	0.0028	0	0
Air-1	0.0514	0.6701	0	0.1551	0.0088	0	0
Hot Air	0.5139	1.9845	0	0.2192	0.0162	0	0
Air-3	0.0753	0.7277	0	0.1588	0.0093	0	0
Air-2	0.0514	0.6701	0	0.1551	0.0088	0	0
Air-4	0.0514	0.6701	0	0.1551	0.0088	0	0
Water	0.0514	0.6701	0	8.3584	7.4518	0	0

The results of the PSCI contains 11 critical streams. Table 2 shows the results after ranking by PSCI. A magnification factor of 100 is used, which can be modified as needed until the PSCI is corrected to the appropriate value. The higher the PSCI value, the more likely the streams are to cause greater damage in case of a leak and lead to different accident scenarios.

According to the physical properties of the analysed flow obtained by HYSYS simulation, the appropriate model is selected and calculated. Since all the analysed streams are in the gas phase, Eq. (19) or Eq. (20) is chosen to calculate the leakage rate of the pipeline. The radiation flux of the jet fire is further calculated based on the leakage rate, which can be used in Eq. (24). Since the radiation flux is diminished with the distance between, the calculated radiation flux located at 0.5m is firstly selected in this paper, and the specific data are shown in Table 3.

Table 3. Radiation flux at 0.5m

Stream name	Leakage rate (kg/s)	Radiation flux (kW/m ²)
Atr top	0.00172	11.9317
Hot methanol	0.00346	135.092
Reform feed	0.00341	33.6328
HTS top	0.00095	5.77462
Gas	0.00079	1.90137
Cooled atr top	0.00104	7.21096
Mixed feed	0.00103	6.52901
LTS top	0.00117	7.00823
LTS feed	0.00122	7.35813
Synsas gas	0.00124	7.38635
Flue gas	0.00072	0.48923

This paper assumes a pipe diameter of 30 mm and a pipe length of 3 mm. Correspondingly, the leakage calibre was chosen to be 0.1 of the pipe diameter, i.e., 3 mm for calculation. By observing the radiation flux of each stream at 0.5m, it can be visualized that high-temperature methanol is ranked first in the consequence assessment. Therefore, in the consequence assessment of each stream, high-temperature methanol possesses a very high risk and may cause very serious consequences if a jet fire occurs.

Since the value of radiation flux changes with distance, it is necessary to discuss the distribution of radiation flux in different locations for each stream. This paper selects the radiation flux of 4 kW/m² as a critical point for analysis and studies the critical distance when the radiation flux of each stream is lower than 4 kW/m². The variation of radiation flux with distance for each stream is shown in Fig. 4-5. Based on the calculated values of radiation flux at 0.5 m for each stream, the initial radiation flux is higher for the methanol high-temperature streams and the reforming feed streams, so the two streams

are analysed separately. The variation of radiation flux with distance for the methanol high-temperature streams is shown in Fig. 4. The methanol contained in this stream occupies a high calorific value, so when a jet fire occurs it has a considerable impact on the surrounding area. The radiation flux only decreases to 4 kW/m² when the environmental distance is located at 4 m. Therefore, it is known that the environmental impact of these streams can reach 4 m. In addition, the feed stream of the reformer also has more serious consequences compared to other streams. The variation of the radiation flux of this stream is also shown in Fig. 4. Compared to the methanol high-temperature streams, this stream has a lower radiation flux at 0.5 m, but the critical value of the radiation flux continues between 1.5 and 2 m. In addition to the radiation fluxes of the above two streams, the radiation fluxes of other streams are presented in Fig. 5. From the figure, it can be seen that all the streams fall below the critical value of radiation flux at about 1 m. Among them, the HT-PEMFC exhaust gas streams and the post-combustion waste stream are even below 4 kW/m² at 0.5 m. Compared with the above two streams, this part of the stream has a lower risk. From Fig. 5, it can be observed that the exit streams of the reformer have a higher hazard, and this stream is also the stream ranked first in the PSCI index.

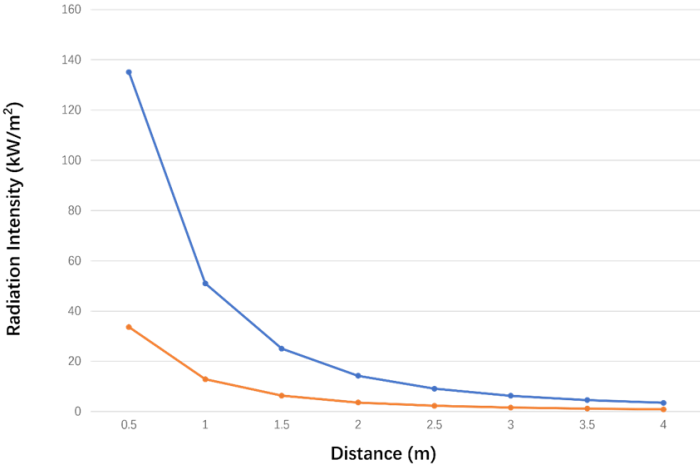


Figure 4. Event tree model with different accident consequences

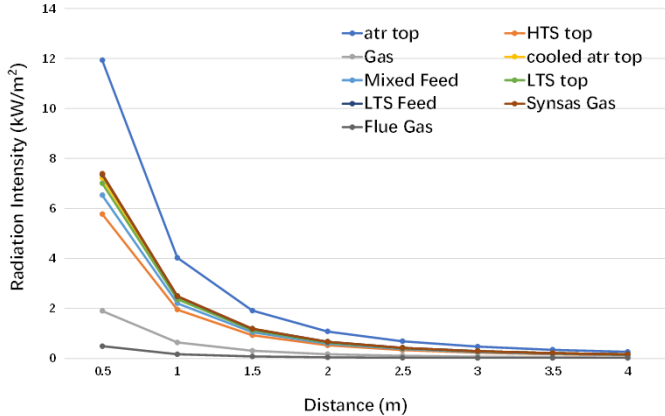


Figure 5. Variation of radiation flux with distance when a jet fire occurs in other 9 streams

According to Eq. (25), to obtain the possibility of jet fire for each stream, it is necessary to calculate the leakage frequency, immediate ignition frequency, delayed ignition frequency, and explosion probability, respectively. The probability of a jet fire occurring in the streams is shown in Table 4.

Table 4. Jet fire probability calculation

Stream name	f_{IL}	$P_{imm,ign}$	$P_{del,ign}$	$P_{exp/g/ign}$	f
Atr top	7.056E-05	1	0.5451	0.0017933	7.0556E-05
Hot methanol	7.056E-05	0.0235	0.5451	0.0024635	3.9122E-05
Reform feed	7.056E-05	0.0235	0.5451	0.0024137	3.9124E-05
HTS top	7.056E-05	0.9139	0.5451	0.0014929	6.7786E-05
Gas	7.056E-05	1	0.5451	0.0013775	7.0556E-05
Cooled atr top	7.056E-05	0.0635	0.5451	0.0015479	4.0444E-05
Mixed feed	7.056E-05	0.0635	0.5451	0.0015441	4.0444E-05
LTS top	7.056E-05	0.0818	0.5451	0.0016306	4.1026E-05
LTS feed	7.056E-05	0.0778	0.5451	0.0016556	4.0899E-05
Synsas gas	7.056E-05	0.0818	0.5451	0.0016676	4.1025E-05
Flue gas	7.056E-05	1	0.5451	0.0013101	7.0556E-05

2.3 Jet Fire Risk Assessment

The risk of an accident is a combination of the consequences of an accident and the likelihood of an accident occurring and is the result of both. By referring to the risk matrix table in Athar's paper[14], the risk level of pipeline jet fire in this paper is determined. Subsequently, based on the determined levels, the level of risk of a jet fire occurring in each stream was determined by consulting the risk matrix. Fig. 6 indicates that the risk level of the whole object is concentrated in the two levels of tolerable and acceptable. There are three higher tolerance levels, which are methanol reformer outlet streams, high-temperature methanol streams, and reformer feed inlets. Most of the other streams are also at tolerable levels at closer locations, where the exhaust gas from the HT-PEMFC and the exhaust gas from the burner are not at high risk over the entire distance due to their low radiation flux when jet fires occur. According to Fig. 6, the three streams with higher risk levels are concentrated around the high-temperature reformer of methanol. Therefore, it is known that for the on-board methanol reforming to hydrogen system, the risk level is higher for the part located around the methanol reformer. The next most dangerous part of the system is the water-vapor conversion part, which is less risky than the methanol reforming part, although the streams in this part are also dangerous.

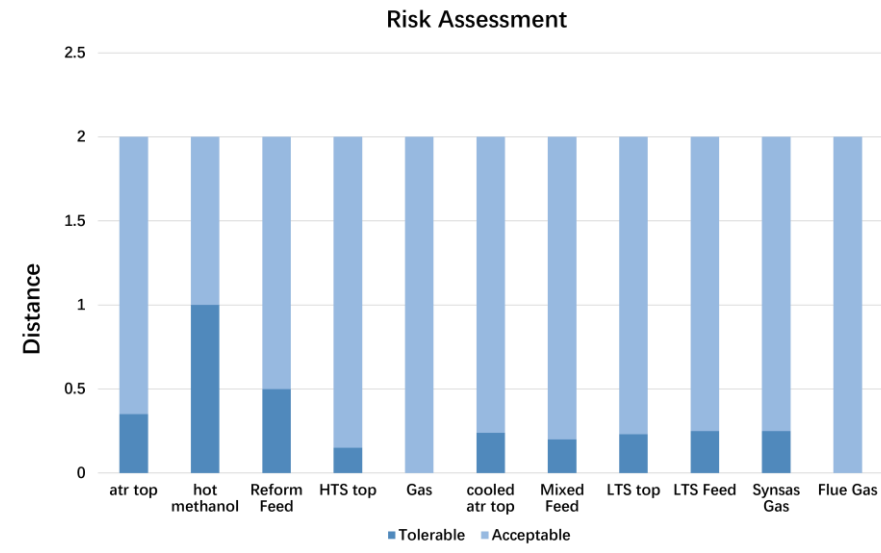


Figure 6. Risk level of each stream

2.4 Calculation of the Consequences and Probability of Vapor Cloud Explosion of Streams

Based on the previous PSCI ranking results, the top five were selected for the VCE risk analysis of the streams in this paper. In the consequence analysis, a breakage scenario was assumed for the pipelines

in this paper to achieve a conservative analysis. Therefore, the inventory within each pipeline is the main reference. Subsequent consequence calculations are made in turn from Eq. (26) to (29), and finally, the distribution of explosion overpressure with distance in the event of a VCE is calculated for each stream. The TNT equivalent method of calculation can be used to initially obtain the equivalent TNT mass in the event of a VCE explosion of the pipeline, the specific data are shown in Table 5.

Table 5. VCE Consequence Parameters for Streams

Tag No	m (kg)	m_f/m	m_{TNT} (kg)
atr top	0.40	0.853036751	0.21
hot methanol	0.12	0.677089138	0.32
Reform Feed	0.40	0.677089138	0.28
HTS top	0.43	0.877191548	0.20
Gas	0.68	0.856163747	0.12

Based on the data requested in Table 5, the equivalent TNT mass at the time of VCE explosion for each device can be obtained. Subsequently, the scaling distance and overpressure level of explosion overpressure at different distances can be calculated using Eq. (28) to Eq. (29). In this paper, the overpressure of the equipment at different distances was calculated using 5m as a scale, and the detailed data of the calculation are shown in Table 6.

Table 6. Scale Distance(m) and Overpressure(kPa) for Streams

Tag No	5m	10m	15m
atr top	21 kpa	9 kpa	4 kpa
hot methanol	26 kpa	12 kpa	5 kpa
Reform Feed	25 kpa	10 kpa	4.7 kpa
HTS top	20 kpa	7 kpa	4 kpa
Gas	17 kpa	6 kpa	3 kpa

After completing the calculation of the explosion overpressure of VCE, the next step is to calculate the probability of VCE explosion occurrence. The specific calculation process is similar to jet fire, using Eq. (30) to calculate the relevant parameter, and the specific calculation results for each device are shown in Table 7.

Table 7. Probability for VCE

Tag No	f_{IL}	$P_{imm,ign}$	$P_{del,ign}$	$P_{exp/g/ign}$	f_{VCE}
atr top	7.056E-05	1	0.545102005	0.0042935	0
hot methanol	7.056E-05	0.02352085	0.545102005	0.0058154	2.184E-07
Reform Feed	7.056E-05	0.02352085	0.545102005	0.0057782	2.17E-07
HTS top	7.056E-05	0.913860003	0.545102005	0.0033213	1.1003E-08
Gas	7.056E-05	1	0.545102005	0.003058	0

3.0 CONCLUSION

In this paper, we have analyzed an on-board methanol reforming system and evaluated the inherent safety of the entire system using the Inherent Safe Process Pipeline (ISPP) method. Based on the

original method, this paper has improved it by adding the consequence assessment of VCE. The findings are as follows.

In the risk assessment of the jet fire, the three streams with higher risk levels are concentrated around the methanol high-temperature reformer. Therefore, it is known that for the on-board methanol reforming hydrogen system, the risk level is higher for the part located around the methanol reformer. This analysis shows that the reformer structure is the more dangerous part of the whole structure for the on-board methanol reforming system streams only.

In the risk assessment of the VCE, although for the pipeline, the possibility of explosion is low, but if it happens will also cause serious consequences. Therefore, the consequences of the explosion in the system should also take certain protection.

REFERENCES

1. Dawood, F., M. Anda, and G.M. Shafiullah, Hydrogen production for energy: An overview. *International Journal of Hydrogen Energy*, 2020. **45**(7): p. 3847-3869.
2. Muradov, N. and T. Vezirolu, From hydrocarbon to hydrogen?carbon to hydrogen economy. *International Journal of Hydrogen Energy*, 2005. **30**(3): p. 225-237.
3. Sun, Z. and Z.-q. Sun, Hydrogen generation from methanol reforming for fuel cell applications: A review. *Journal of Central South University*, 2020. **27**(4): p. 1074-1103.
4. Sazali, N., et al., New Perspectives on Fuel Cell Technology: A Brief Review. *Membranes (Basel)*, 2020. **10**(5).
5. Chein, R., et al., Design and test of a miniature hydrogen production reactor integrated with heat supply, fuel vaporization, methanol-steam reforming and carbon monoxide removal unit. *International Journal of Hydrogen Energy*, 2012. **37**(8): p. 6562-6571.
6. Kolb, G., et al., Design and operation of a compact microchannel 5 kW el,net methanol steam reformer with novel Pt/In 2 O 3 catalyst for fuel cell applications. *Chemical Engineering Journal*, 2012. **207-208**: p. 388-402.
7. Yang, M., et al., A self-sustained, complete and miniaturized methanol fuel processor for proton exchange membrane fuel cell. *Journal of Power Sources*, 2015. **287**: p. 100-107.
8. Ghodba, A., M. Sharifzadeh, and D. Rashtchian, Integrated and inherently safe design and operation of a mobile power generation: Process intensification through microreactor reformer and HT-PEMFC. *International Journal of Hydrogen Energy*, 2021. **46**(46): p. 23839-23854.
9. Park, S., et al., Incorporating inherent safety during the conceptual process design stage: A literature review. *Journal of Loss Prevention in the Process Industries*, 2020. **63**.
10. Khan, F.I. and P.R. Amyotte, I2SI: A comprehensive quantitative tool for inherent safety and cost evaluation. *Journal of Loss Prevention in the Process Industries*, 2005. **18**(4-6): p. 310-326.
11. Rathnayaka, S., F. Khan, and P. Amyotte, Risk-based process plant design considering inherent safety. *Safety Science*, 2014. **70**: p. 438-464.
12. Leong, C.T. and A.M. Shariff, Process route index (PRI) to assess level of explosiveness for inherent safety quantification. *Journal of Loss Prevention in the Process Industries*, 2009. **22**(2): p. 216-221.
13. Shariff, A.M., C.T. Leong, and D. Zaini, Using process stream index (PSI) to assess inherent safety level during preliminary design stage. *Safety Science*, 2012. **50**(4): p. 1098-1103.
14. Athar, M., et al., Inherent safety for sustainable process design of process piping at the preliminary design stage. *Journal of Cleaner Production*, 2019. **209**: p. 1307-1318.